

First-order transition between a small-gap semiconductor and a ferromagnetic metal in the isoelectronic alloys $\text{FeSi}_{1-x}\text{Ge}_x$

V. I. Anisimov^{1,2}, R. Hlubina^{1,3}, M. A. Korotin², V. V. Mazurenko^{1,2}, T. M. Rice¹, A.O.Shorikov^{1,2}, M. Sigrist¹

¹*Institute for Theoretical Physics, ETH Hönggerberg, CH-8093 Zürich, Switzerland*

²*Institute of Metal Physics, Russian Academy of Sciences, 620219 Yekaterinburg GSP-170, Russia*

³*Department of Solid State Physics, Comenius University, Mlynská Dolina F2, 842 48 Bratislava, Slovakia*

The contrasting groundstates of isoelectronic and isostructural FeSi and FeGe can be explained within an extended local density approximation scheme (LDA+U) by an appropriate choice of the onsite Coulomb repulsion, U on the Fe-sites. A minimal two-band model with interband interactions allows us to obtain a phase diagram for the alloys $\text{FeSi}_{1-x}\text{Ge}_x$. Treating the model in a mean field approximation, gives a first order transition between a small-gap semiconductor and a ferromagnetic metal as a function of magnetic field, temperature, and concentration, x . Unusually the transition from metal to insulator is driven by broadening, not narrowing, the bands and it is the metallic state that shows magnetic order.

The unusual magnetic susceptibility of FeSi has been a subject of interest for a long time. Jaccarino *et al.*¹ found a rapid crossover around room temperature from activated behavior at low temperature to an apparent localized Curie-Weiss form at high temperature. This has stimulated a number of proposed explanations. Among them are a form of Kondo insulating behavior in FeSi ^{2,3}, although an underlying microscopic model has not been clarified, and almost ferromagnetic semiconductor model^{4,5}. The latter received support from the detailed LDA band structure calculation of Mattheiss and Hamann⁶. They found a small gap semiconductor with formal neutral valences Fe^{0+} , Si^{0+} on both elements. Later Anisimov *et al.*⁷ extended these calculations to include the onsite Coulomb interaction, U , in a mean field approximation, the so-called LDA+U method⁸, and found, for a reasonable choice of U , a ferromagnetic metallic phase very close by in energy. This led them to propose that a transition to this ferromagnetic state could be driven by applying a magnetic field (B) and that the unusual temperature (T) dependent susceptibility in FeSi reflected the proximity to a critical point of this transition at finite (B_c , T_c). However the predicted value of B_c ($\approx 170\text{T}$) is too large to be reached in the laboratory and the existence of the critical point remains untested experimentally. A non-trivial prediction was the fractional value of the saturation moment of the ferromagnetic phase at $S = 1/2$ or $1 \mu_B/\text{Fe}$. This is a consequence of the band structure and cannot be reconciled with a local model and a $3d^8$ configuration for Fe^{0+} .

The magnetic properties of the isoelectronic and isostructural FeGe compound have aroused less interest. It is a magnetic metal with a long period spiral form which is simply a ferromagnet twisted by the Dzyaloshinskii-Moriya interaction that is a consequence of the absence of inversion symmetry at the Fe site in this cubic structure¹⁰. Interestingly the saturation moment is

the fractional $S = 1/2$ value quoted above^{11,12}. In this letter we report LDA+U calculations (in TBLMTO calculation scheme⁹) for FeGe and the isoelectronic alloys $\text{FeSi}_{1-x}\text{Ge}_x$. Motivated by these results we use a simplified phenomenological model to explore the complete phase diagram of the isoelectronic alloys $\text{FeSi}_{1-x}\text{Ge}_x$ with varying T and B . Alloying FeSi with Ge allows one to tune the predicted semiconductor to ferromagnetic metal transition and its unusual critical point at (B_c , T_c), to experimentally convenient values.

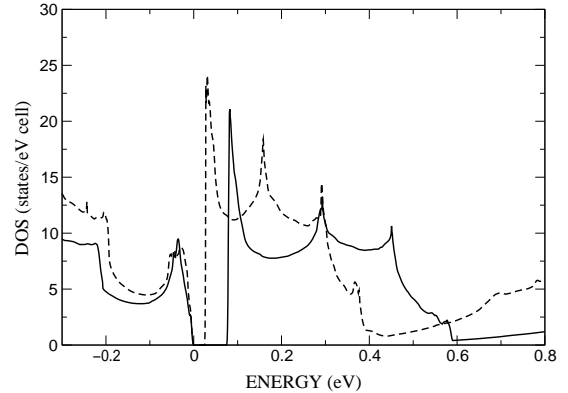


FIG. 1: The density of states (DOS) near the Fermi level at zero energy obtained from LDA calculations. The solid and dashed lines represent FeSi and FeGe with energy gaps 0.08 eV and 0.03 eV respectively. The corresponding widths of the peaks above the Fermi level are 0.5 eV and 0.37 eV .

Both FeSi and FeGe crystallize in the cubic B20 structure which can be viewed as highly distorted rocksalt with 4 FeSi formula units in the primitive cell. Each Fe site has 7 Si neighbors and point group symmetry, C_3 . The LDA band structure calculations of Mattheiss and Hamann⁶ place the Fermi energy within a narrow manifold of 20 bands of predominantly Fe $3d$ charac-

ter lying within a larger hybridization gap with the Si ($3p$, $3s$) states. A fuller description of the band structure will be presented elsewhere¹³. A nontrivial feature of their results is the presence of a small but complete band gap separating 16 filled valence bands from 4 empty conduction bands. The conduction bands have nonbonding character with respect to the Si atoms and are divided by a pseudogap into two lower lying quite narrow bands and two higher lying bands which are much wider. The results of our LDA band calculations for FeGe are similar but with an even smaller band gap and narrower overall bandwidths as expected from the larger lattice constant. The total density of states for both compounds is shown in Fig. 1.

Anisimov et al.⁷ extended the LDA calculations for FeSi to incorporate the onsite Coulomb repulsion (U) on the Fe-sites in a mean field approximation scheme known as LDA+U⁸. They found a local minimum in the total energy versus magnetization at a value $\approx 1\mu_B/\text{Fe}$ which moved to lower energy with increasing U . In this magnetized state the lower pair of conduction bands are filled for the majority spin direction while the Fermi level of the minority spin electrons lies in the valence band complex leading to metallic behavior. The relative positions of the two minima corresponding to the small gap semiconductor and magnetized metal, depends on the choice of U which is not known precisely.

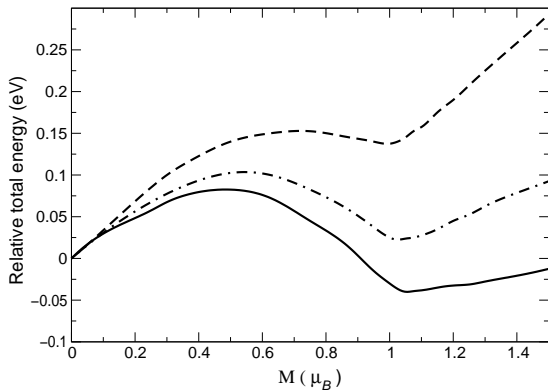


FIG. 2: The evolution of the total energy (with energy of nonmagnetic solution taken a zero) as a function of the spin moment $M(\mu_B/\text{Fe})$ for the value of $U = 3.7\text{eV}$. The solid, dashed and dashed-dotted lines correspond to FeGe, FeSi and $\text{FeSi}_{0.58}\text{Ge}_{0.42}$ respectively.

We have used the TBLMTO scheme⁹ to perform LDA+U calculations for FeGe. The narrower bandwidths and energy gap lead to a lower value for the critical U , where the two energy minima cross, in FeGe relative to FeSi. Thus it is possible to obtain within the LDA+U scheme for a common value of U , the correct groundstates for FeSi and FeGe¹⁴ (see Fig. 2). There are two unusual aspects to this metal-insulator transition (MIT). It is the metallic state, rather than the insulating

state, which is magnetically ordered. Secondly, the transition from insulating to metallic behavior is driven by narrowing, rather than increasing, the bandwidth. The inverted nature of the metal-insulator transition is a direct consequence of the fact that the MIT is driven by the paramagnet-ferromagnet transition.

FeSi and FeGe are the end members of the isoelectronic and isostructural alloys, $\text{FeSi}_{1-x}\text{Ge}_x$. We have extended the LDA+U calculations to the alloys¹⁵ using experimental lattice parameters¹⁶. The critical value x_c of the first order transition is sensitive to the choice of U . For the value of $U = 3.7\text{eV}$, illustrated in Fig. 2, $x_c = 0.4$ in a good agreement with the experimental value $x_c = 0.3$ ¹⁶.

To proceed further we introduce and solve (within a mean field approximation) a minimal phenomenological model for the isoelectronic alloys $\text{FeSi}_{1-x}\text{Ge}_x$. Motivated by the experimental fact that the ordered moment in FeGe is $\approx 1\mu_B$ per Fe atom^{11,12} which implies a fractional magnetization with respect to the paramagnetic $\text{Fe } 3d^8$ configuration, we are led to an itinerant model of magnetism. We consider the following model for the conduction and valence bands. The valence band, describing the upper part of the manifold of occupied $\text{Fe } 3d$ bands, stretching below zero energy in Fig. 1, has a width $2W$ and contains one state per spin per Fe atom. The conduction band (of width W) contains $1/2$ -state per spin per Fe atom and when multiplied by 4 (which is the number of Fe atoms per primitive cell), it corresponds to the two narrow conduction bands just above the Fermi level. Both the valence and conduction bands are assumed for simplicity to have a constant density of states $N(\varepsilon) = (2W)^{-1}$ per spin, with a \mathbf{k} -independent gap of 2Δ . Taking 2 conduction electrons per Fe atom, leads to a fully occupied valence band and a semiconducting ground state in the noninteracting case.

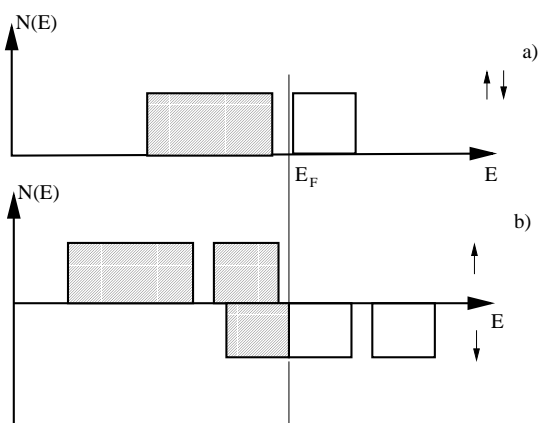


FIG. 3: Density of states of the model band structure. (a) Nonmagnetic semiconducting state. (b) Magnetic metallic state. The arrows note majority and minority spins.

We propose that three types of effective local interactions should control the physics: intraband repulsion \tilde{U} ,

interband repulsion V , and exchange coupling between the bands I . The interactions \tilde{U} , V , and I are combinations of the matrix elements of the Coulomb interaction between the relevant Wannier orbitals and are taken as a phenomenological input to our theory. Furthermore, we assume that the primary effect of the \tilde{U} term is to strongly renormalize the bandwidth W with respect to estimates from the LDA calculations. In order to describe the experimental data, we have therefore decided to use a phenomenological bandwidth rather than the calculated $W \sim 0.5$ eV⁶. Thus, in order not to double count its effects, the \tilde{U} term is not included in our model Hamiltonian which reads

$$H = \sum_{\lambda, \mathbf{k}, \sigma} (\varepsilon_{\lambda \mathbf{k}} - \sigma \mu_B B) n_{\lambda \mathbf{k} \sigma} - \frac{1}{2} \sum_{\mathbf{R}} (I \hat{m}_{\mathbf{R}}^2 + V \hat{\rho}_{\mathbf{R}}^2),$$

where $\lambda = -1, +1$ denotes the valence and conduction bands, respectively, and $\varepsilon_{\lambda \mathbf{k}}$ and $n_{\lambda \mathbf{k} \sigma}$ is the band energy and number of electrons with momentum \mathbf{k} and spin σ in band λ . The operators $\hat{\rho}_{\mathbf{R}} = 2 + \sum_{\lambda \sigma} \lambda n_{\lambda \mathbf{R} \sigma}$ and $\hat{m}_{\mathbf{R}} = \sum_{\lambda \sigma} \sigma n_{\lambda \mathbf{R} \sigma}$ measure the local number of charge carriers and the local magnetization, respectively. The spin quantization axis has been chosen in the direction of the external magnetic field B . The Hamiltonian can be written also in an explicitly spin-rotation invariant form, which we do not specify here.

Below we describe the phase diagram of the $\text{FeSi}_{1-x}\text{Ge}_x$ alloys by fixing the values of I , V , and Δ irrespective of the Ge content x . Alloying changes the bandwidth W which decreases with increasing x , in accordance with the LDA results. Treating the interaction terms in the mean field approximation allows to replace the operators $\hat{\rho}_{\mathbf{R}}$ and $\hat{m}_{\mathbf{R}}$ by the expectation values ρ and m , respectively. The main technical difference of the present study with respect to Ref. 7 is that our model is not particle-hole symmetric, and therefore in addition to m and ρ , the chemical potential μ has to be calculated self-consistently. Assuming finite values of m and ρ , the single-particle energies in the lower and upper bands are $\omega_{\lambda, \sigma} = \varepsilon - \lambda V \rho - \sigma (\mu_B B + I m)$. The corresponding mean particle numbers are

$$\langle n_{-, \sigma} \rangle = (2W)^{-1} \int_{-\Delta-2W}^{-\Delta} \frac{d\varepsilon}{1 + \exp(\omega_{-, \sigma} - \mu)/T}, \quad (1)$$

$$\langle n_{+, \sigma} \rangle = (2W)^{-1} \int_{\Delta}^{\Delta+W} \frac{d\varepsilon}{1 + \exp(\omega_{+, \sigma} - \mu)/T}. \quad (2)$$

The equation for the total number of particles $2 = \sum_{\lambda, \sigma} \langle n_{\lambda, \sigma} \rangle$ together with Eqs. (1,2) form a closed set of equations for ρ , m , and μ , which have to be solved in general numerically.

At $T = 0$, the model can be solved analytically. For sufficiently large bandwidth W , the following two phases compete: (i) semiconductor with $\rho = 0$, $m = 0$ and (ii) ferromagnetic metal with $\rho = 1$, $m = 1$. Their energies are $E_{\text{semi}} = -2\Delta - 2W$ and $E_{\text{FM}} = -\Delta - 3W/2 -$

$(I + V)/2 - \mu_B B$, respectively. With changing bandwidth, at $B = 0$ there is a level crossing between the semiconducting phase and the ferromagnetic metal at $W = W_c(0) = I + V - 2\Delta$. For $W > W_c(0)$, the ferromagnetic phase is stable only in magnetic fields larger than a critical magnetic field $\mu_B B_c(0) = (W - W_c(0))/2$.

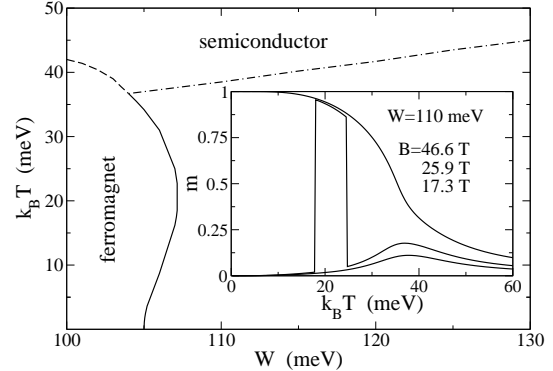


FIG. 4: Phase diagram in the W - T plane at $B = 0$. The semiconductor-ferromagnet transition (solid line) is of first order at low temperatures, up to a critical point at $W_c \approx 104$ meV and $T_c \approx 37$ meV. At higher temperatures, the transition is of second order (dashed line). The spin susceptibility in the paramagnetic phase peaks at temperatures indicated by the dash-dotted line. The inset shows the magnetization as a function of temperature for a nearly critical alloy composition in an applied magnetic field.

We take $\Delta = 20$ meV in qualitative agreement with experiment and the effective interaction parameters $I = 80$ meV and $V = 65$ meV close to the values proposed in Ref. 7. The resulting phase diagram for $B = 0$ shown in Fig. 4 implies that the phenomenological bandwidth of FeGe, W_{FeGe} , is less than $W_c(0)$ ($W_c(0) = 105$ meV). Note that the Curie temperatures predicted by our model for $W < W_c(0)$, $T_c \sim 400$ K, are in reasonable agreement with the experimentally observed transition temperature to a long-period spiral in FeGe, $T_N \approx 280$ K¹⁰. The phenomenological bandwidth of FeSi, W_{FeSi} , which is greater than $W_c(0)$, can be determined by fitting the spin susceptibility. For $W \geq W_c(0)$, the spin susceptibility develops a strong peak around room temperature, confirming the interpretation of Anisimov *et al.* The peak position as a function of W is shown in Fig. 4. Fitting the peak value of χ to $\approx 27\mu_B^2/\text{eV}^1$, we estimate $W_{\text{FeSi}} \approx 130$ meV.

Nearly critical semiconducting alloys with W slightly in excess of $W_c(0)$ should exhibit metamagnetic transitions to metallic phases at experimentally accessible magnetic fields. For instance in a sample with $W = 110$ meV, the transition occurs at $B_c(0) = 43.1$ T at $T = 0$. The temperature evolution of the magnetization m for such a sample for magnetic fields in the vicinity of the first-order transition is shown in the inset in Fig. 4. Note that at low temperatures the critical magnetic field lowers with increasing temperature. This follows simply from the larger electronic entropy of the metallic phase. At higher

temperatures the phase boundary in our model bends towards smaller bandwidths W , in qualitative agreement with the higher susceptibility of small bandwidth systems to various forms of symmetry breaking transitions. The different low- and high- T slopes of the phase boundary lead to a reentrant $B = 0$ phase diagram and also to reentrant metamagnetic transitions in a narrow field range, as shown explicitly in the inset in Fig. 4 for $B = 25.9$ T.

We should like to point out that not only the magnetic properties are anomalous at the metamagnetic transition. Since the transition is between a *semiconductor* and a ferromagnetic *metal*, large magnetoresistance is to be expected. As a result the critical endpoint of this metamagnetic transition should show particularly interesting magnetoresistance behavior at temperatures around room temperature.

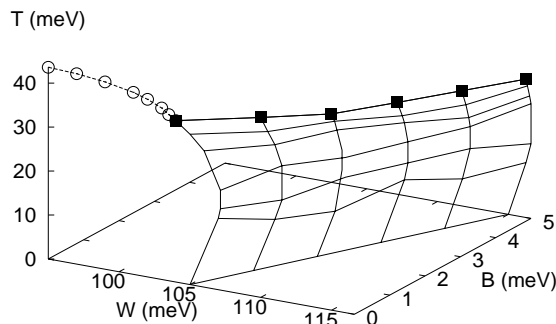


FIG. 5: Complete phase diagram of the isoelectronic alloys $\text{FeSi}_{1-x}\text{Ge}_x$. The semiconducting phase at large bandwidths W (small Ge content x) is separated from the ferromagnetic metal phase at small W (large x) by a surface of first-order transitions terminating in a line of critical points (solid squares) around the room temperature. At $B = 0$ and at Curie temperatures which lie above the temperature of the critical point, there is a second-order phase transition between the paramagnetic and ferromagnetic phases (open circles).

In conclusion, we have calculated the complete phase diagram of the isoelectronic alloys $\text{FeSi}_{1-x}\text{Ge}_x$ with varying T and B . Our main results are summarized in a three-dimensional phase diagram, Fig. 5, which shows that, depending on x , T , and B , the alloy $\text{FeSi}_{1-x}\text{Ge}_x$ can be a semiconductor or a ferromagnetic metal. The two phases are separated by a surface of first-order transitions which terminates at high temperatures in a line of critical points. Note, this phase diagram resembles that found by Pfleiderer *et al.*¹⁷ for isostructural MnSi under pressure and magnetic field but with the important difference that all phases of MnSi are metallic so that a semiconductor-metal transition is not involved. We pre-

dict that, for intermediate values of the Ge content x , this transition can be realized as a metamagnetic transition at experimentally accessible magnetic fields. Large magnetoresistance is predicted at such a transition. Another possible way to realize the transition at experimentally accessible magnetic fields would be to apply pressure to FeGe .

VIA, VVM, AOS and RH thank the Center for Theoretical Studies, ETH Zurich and the Swiss National fond for support. Partial support by the Slovak Grant Agency VEGA under Grant No. 1/9177/02 and Russian Foundation For Basic Research grant RFFI-01-02-17063 is also acknowledged. We are especially grateful to Zachary Fisk for pointing out the experimental results on FeGe to us and for communicating his unpublished results on the $\text{FeSi}_{1-x}\text{Ge}_x$ alloys.

- ¹ V. Jaccarino *et al.*, Phys. Rev. **160**, 476 (1967).
- ² T. Mason *et al.*, Phys. Rev. Lett. **69**, 490 (1992).
- ³ D. Mandrus *et al.*, Phys. Rev. B **51**, 4763 (1995).
- ⁴ Y. Takahashi and T. Moriya, J. Phys. Soc. Jpn. **46**, 1451 (1979).
- ⁵ S. N. Evangelou and D. M. Edwards, J. Phys. C **16**, 2121 (1983).
- ⁶ L. F. Mattheiss and D. R. Hamann, Phys. Rev. B **47**, 13 114 (1993).
- ⁷ V. I. Anisimov, S. Yu. Ezhov, I. S. Elfimov, I. V. Solovyev, and T. M. Rice, Phys. Rev. Lett. **76**, 1735 (1996).
- ⁸ V.I. Anisimov, J. Zaanen and O.K. Andersen, Phys. Rev. B **44**, 943 (1991); Vladimir I. Anisimov, F. Aryasetiawan, A.I. Lichtenstein, J. Phys.: Condens. Matter **9**, 767 (1997).
- ⁹ O.K. Andersen, and O. Jepsen, Phys. Rev. Lett. **53**, 2571 (1984). O.K. Andersen, Z. Pawłowska, and O. Jepsen, Phys. Rev. B **34**, 5253 (1986)
- ¹⁰ B. Lebech, J. Bernhard, and T. Freltoft, J. Phys.: Condens. Matter **1**, 6105 (1989).
- ¹¹ R. Wäppling and L. Häggström, Physics Lett. **28A**, 173 (1968).
- ¹² L. Lundgren, K. Å. Blom, and O. Beckman, Physics Lett. **28A**, 175 (1968).
- ¹³ V.I.Anisimov *et al* (to be published).
- ¹⁴ Because of the neglect of spin-orbit coupling in these calculations, the Dzyaloshinskii-Moria interactions which cause the long period spiral order in FeGe , are not included and ferromagnetic order results.
- ¹⁵ The electronic structure of $\text{FeSi}_{1-x}\text{Ge}_x$ alloys was calculated in the approximation, where in TBLMTO calculation scheme⁹ the potential parameters for non-metallic atoms were taken as the corresponding average of the Si and Ge parameters.
- ¹⁶ Z.Fisk (private communication)
- ¹⁷ C.Pfleiderer, S.R.Julian and G.G.Lonzarich, Nature **414**, 427 (2001)